

Performance Analysis of Double Gate Dielectric Modulation In Schottky FET As Biomolecule Sensor

Prasahanth Kumar (✉ prash.034@gmail.com)

Vellore Institute of Technology (VIT) <https://orcid.org/0000-0002-2448-8341>

Research Article

Keywords: Schottky barrier (SB), nanogap region, charge-plasma, dielectric constant, biomolecules, double gate

Posted Date: May 11th, 2021

DOI: <https://doi.org/10.21203/rs.3.rs-491889/v1>

License:  This work is licensed under a Creative Commons Attribution 4.0 International License.

[Read Full License](#)

Version of Record: A version of this preprint was published at Silicon on July 16th, 2021. See the published version at <https://doi.org/10.1007/s12633-021-01197-y>.

Abstract

In this article, a charge-plasma (CP)-based double gate schottky barrier FET structure has been investigated using dielectric controlled biomolecule sensor. The use of Hafnium as a charge plasma at the source side encourages an n+ charge plasma in an un-doped silicon region, which expressively decreases the Schottky barrier thickness. The oxide below the Metal gate M_1 and M_2 is etched out to create nanogap openings for biomolecule finding. Here, the existence of molecules is categorized by the modification in oxide material inside the nanogap and the related charge densities, hence, to controls the tunneling thickness at the Metal-source-silicon channel interface, also with the help of plasma charges in an intrinsic-Si film. This paper is mainly focused on the fundamental physics of the proposed structure and approximations of their relative sensitivity detecting enactment. The sensing enactment has been assessed for charged biomolecules and charge-neutral biomolecules by widespread device simulation, and the special properties of the biomolecule. The proposed device improves its control over the tunneling region and this has been used for the sensing, ensuing to larger on-state drain current (I_{ds}) sensitivity for biomolecule. Hence, the gate voltage is recognised as the active design parameters for efficient reduction. Moreover, the sensing of the SB FET-based biosensor threshold voltage (V_{th}), abnormality in the on-current (I_{on}), and I_{on}/I_{off} ratio has been shown. Also, the charge-plasma (CP)-based double gate schottky barrier FET simulations calibrated with experimental results. Hence, the relative change in I_{on} using charge-plasma (CP)-based double gate schottky barrier FET biosensor maintain improved detecting ability for biomolecule recognition.

Introduction

In the earlier, research significant exploration has been absorbed on silicon-film based FET biosensors owed to the capable features of great sensitivity, smallest delay, scaled sizes and minimum cost [1–4]. The FET-based biosensors have the restriction of thermal electron emission and have a contact resistance and fabrication cost can be more [5]. Due to that schottky tunneling mechanism is preferred, the schottky barrier (SB)-FET modified the restriction and drops the short channel effect [6–8]. Later, SB-FET-based biosensor has appeared as an appropriate applicant for improved sensitivity and response time than MOSFET-based biosensor [9–11]. The simple working of a Schottky barrier (SB) field-effect transistor (FET) conventional biosensor is to moderate the electrical properties with gate bias over the combination of objective biomolecules, then calculating the improved electrostatic enactment limitations. Such conventional SB-FET enactment limitations naturally contain the capacitance, I_{on} -current, transconductance and threshold voltage [12]. The benefits of sensing conventional biosensors contain their scope of on-chip integration, scalability, and low power dissipation [13]. The sensing of conventional device is critical and advanced sensing near the objective biotic species identifies greater ability. The dielectric moderated conventional schottky device is measured as unique capable of schottky-tunneling-based biosensors, have the ability to sensing both charge-neutral as well as charge biotic types. The modulation of dielectric in conventional device includes a nanogap under the gate-metal region or in the gate-dielectric. The abnormality of capacitance established on dielectric constant (k) and charge-density

(ρ) of the biomolecules [14]. The conventional devices are developed as the conceivable extra for numerous gate-metal planned metal oxide semiconductor FETs due to their greater enactment in relations to subthreshold swing, power dissipation, and speed. Such greater enactment of SB-FET has been recognised by its schottky carrier tunneling electron transport [15, 16]. Therefore, the enlargement of SB-FET- biosensors for label-free tenders with greater sensitivity and lesser retort time is drawing extra consideration in the latest days. The modulated dielectric SB-FET established biosensor has been described newly by joining the benefits of modulating the dielectric with the essential advantage of SB-FET- created by biosensors. Though, there are insufficient rumours study on the influence of structural adjustments on the sensing enactment of SB-FET. The modified SB-FETs, construction has exposed extensive possibilities for controlling the transfer characteristics and thus refining the subthreshold swing of SB-FET.

Further, the research actuality motivated on surmounting power supply with the decrease in lower channel effects [6], modulation of dielectric in SB-FET -based biosensor has fixed the care on the research. The SB-FET based sensor uses the idea of charge plasma technique to improve the sensing ability of the SB-FET. So far, the possible benefits of SB FET- sensors have only been imitated in hypothetical consideration with no fabrication protests. Moreover, Charge plasma creation in an SB-FET involves great thermal-budget, and carrier flow conferring are high -temperature practices. In this conventional design, the additional boundary in SB-FET having distress in discovering the unexpected doping shape at metal-silicon and silicon-metal interfaces due to the flow of electronics from metal as a source to silicon to the metal as a drain. This grades in a rise in the chance of dopant variations which might differ the sensitivity of the SB -FET from the expected outcomes. Additionally, destructive reducing the dimensions in these SB-FET has caused bigger S/D contact resistance [17]. Later, for imminent reducing the dimensions of SB-FET-sensors in the nano rule. The use of metal-silicide as source and drain will offer a hopeful solution to the chain resistance difficulty. The metal as source and drain are included suddenly and, therefore, removes the condition of doping contour in SB-FET. Further, in CMOS- harmonious, offers improved scalability and needs moderately lesser temperature for S/D creation nearly 600 C [18]. In the opinion of the said problems, the proposed charge plasma-based dielectric variation Schottky barrier FET as a potential structure and examine it for sensing application of charged and charged neutral biomolecules. The proposed structure has a lightly doped p-type Si channel, metal-source–drain regions, and hence, is clear after doping- matters. The nanogap hollows by imprint out the oxide beneath the metal. Similarly, for the right time, SB FET diminishing is mainly due to the creation of charge plasma has been used as a technique to possibly notice the impartial as well as charged biomolecules. The schottky barrier diminishing grades in current variation by altering the drain current section due to the schottky tunneling through the schottky barrier, whereas the drain current section by thermionic emission completed the barrier rests natural. The proposed biosensor improved device characteristics. The sensitivity improvement of the proposed SB-FET biosensor for neutral and charged biomolecules are examined.

Device Structure And Simulation Setup

The schematic using charge plasma-based dielectric variation schottky barrier-FET biosensor device is shown in Fig. 1. The proposed biosensor contains metal Source/Drain junctions, with charge plasma near the source region, an intrinsic Silicon channel with acceptor doping $N_a = 1 \times 10^{15} \text{ cm}^{-3}$. The dual metal double-gate design is measured its device near simulation is fine recognized. By calculation, the dual metal function concurrently in a double metal gate architecture and capably improve the influence of the biomolecule using charge density - dielectric constant, foremost to greater sensing of the biosensors. To attain advanced carrier tunneling, the higher barrier height is considered near the source region. The gate length of dielectric variation SB-FETs is considered as 45 nm. The lateral distance of metal-source and metal-drain regions is 15 nm both and the depth of the silicon-channel is measured as 10 nm. The nanogap region, shown in Fig. 1, is prepared by succeeding the fabrication stages described in [18]. A 2-nm dense HfO₂ deposit inside the nanogap region performances as dielectric to avoid the leakage current at metal-gate to silicon region brought compassion deprivation. The n-type channel SB-FETs device simulations are achieved using Silvaco T-CAD, a commercially accessible device emulator [19]. The thickness gradient imitation model has been used to contain the properties of dimension quantization on the electron transference as well as for better conjunction in the mathematical imitation. The dynamic tunneling model as the nonlocal path is combined to approximation the tunneling module. This model energetically calculates the band-to-band tunnelling (BTBT) lane from the conduction and valence band contour [19]. The horizontal tunnelling width is measured at a deepness of 0.15 nm after the surface, where BTBT is high at the silicon surface. This research is achieved for a selection of the charge density (ρ) and dielectric constant (K) as objective biomolecules inside the range of cavity region. The charge density (ρ) and dielectric constant (K) are selected from the resulting [18], preserving a constant change among the following (ρ) and (K) values for the improved performance. Further, the whole region is filled up with the nanogap region by the biomolecules has been expected. The individual single material constraint of attention, using first with dielectric constant and next with charge density, is measured to fluctuate individual to detect its individual outcome on the sensing property of the sensor. The meshing approach has been measured nonuniformly to make a change from one region of material to an alternative and a moderately thicker meshing has been selected at the edge. Though, the meshing approach is preferred sensibly so that the calculation time is inside the suitable range.

A 2-Dimensional device simulation study is achieved with the silvaco T-CAD simulator [19]. In device simulation, the Lombardi motion method is used to internment the electric field and doping absorption-reliant on mobility. Also, drift-diffusion is included for internment the conveyance practice of electrons. Universal Schottky Tunneling model is involved to detention the electron tunneling near the schottky junction [18], [19]. Shockley-Read-Hall and AUGER techniques have activated the recombination of minority carrier. Fermi-Dirac statistic, and band-gap reduction, model is involved. Similarly, for precise relative study, the simulation of the device is executed by the identical limitations and method for together experimental and proposed structures. Using the charge plasma-based dielectric variation schottky barrier-FET, typical parameters are mainly adjusted to compare the transfer characteristics by repeating the fabrication outcome in Fig. 2, as compared in our work [20]. A respectable promise among fabricated and device simulator outcome was attained. A stable charge density at the oxide interface is

familiarized to replicate the outcome of a charged biomolecule in the dielectric region. Here, a simple operation of the charge plasma-based dielectric variation SB-FET biosensor diminishing by variation in the charge densities and the related dielectric constants as biomolecules in the nanogap hollow region. On behalf of a cavity filled by air-gap ($K = 1$), schottky is extreme though the biomolecules are familiarized in the nanogap region, when K greater than one, schottky width surprises to decrease, with the enlarged capacitance. Further, it can also be implicit as the rise in density of electrons below the charge plasma outstanding to the creation of tunneling. Also in Fig. 2 shows the energy band diagram of the charge plasma based dielectric variation schottky barrier –FET. The energy band shows the on-state condition taking $V_{gs} = 0.8$ V and $V_{ds} = 0.8$ V. The thinning of schottky barrier linked with the electron plasma charges of great density being formed by the Hafnium oxide near-source region [21, 22].

Figure 3 shows the conduction band energy using charge plasma based dielectric variation SB –FET as biosensors by varying different dielectric constants and charge densities of the biosensor, correspondingly. It must be noticeable that the conduction band have been shown at $V_{ds} = 0.8$ V and $V_{gs} = 0.8$ V. In common, to the event of the biomolecule, the transfer of electrons in schottky energy band twisting increases, with a decrease in tunneling length. The conduction band in Fig. 3(a) shows the variance in tunneling of conduction band tinning by using charge plasma based dielectric variation in the proposed device decreases with growing dielectric constants of the biomolecule models. Moreover, Fig. 3(b) shows the rises in complex negative charge density of the biomolecules. Later the biomolecule, in the proposed device gate-to-channel connection decrease is the maximum in the proposed device, the accomplished variance in the tunneling of conduction band twisting among the biosensors is also maximum. Then, the biomolecule in the proposed device hints to superior modification in the thinning conduction band, and thus, a larger variation in the smallest tunneling length is possible.

Further, the effects are exposed in relations to the smallest tunneling length, as plotted for the dielectric-constant keeping charge density $\rho = 0$ for biomolecule models shown in Fig. 4 correspondingly. Such change in tunneling at $V_{ds} = 0.5$ V the proposed device shows improved drain current compassion at quite lesser drain bias. The definitive environment of smallest tunneling width obeyed for conduction-band with biomolecules as a dielectric.

For evolving an improved thoughtful on the qualified routine of the proposed device, it is critical to experience proportional learning on the bias need of the tunneling interface in biosensors. The efficiency of the dielectric constant on the tunneling region can be measured by a constraint clear as electrostatic potential sensitivity, $S\phi$, given by.

$$S\phi = \left(\frac{\phi_s^{bio} - \phi_s}{\phi_s} \right)$$

The advanced potential compassion, better will be the result of biomolecule over tunneling region where φ_s and φ_s^{bio} are the electrostatic potentials earlier and later biomolecule, correspondingly. Hence, it is obvious that advanced electrostatic potential superior will be the effect on biomolecule sensing schottky region. Later, the effect of tunneling region on the electrostatic potential difference with gate bias ($V_{gs} = 0.8$ V) and drain bias ($V_{ds} = 0.8$ V) has been examined the sensitivity. In general, the electrostatic potential rises with the rise of both gate and drain bias shown in Fig. 5. Figure 5(a, b) shows the variation of dielectric constants keeping charge density as (ρ) = 0 and variation of charge densities, respectively. The electrostatic potential has reduced in the nonappearance of biomolecules ($K = 1$), and later, with a growing dielectric constant greater than k , shows a superior connection between the silicon channel and the source region. Moreover, the negative charge density in the nanogap region rises in the horizontal band.

The simulation of drain current with change gate bias for a proposed device with the impact of dielectric constant as biomolecules taking $k = 1, 4$ and 10 at $V_{ds} = 0.8$ V for completely occupied nanogaps are shown in Fig. 6. Figure 6 at $k = 1$ signifies the current characteristics, after the cavity-region is occupied by air shows a low drain current compared to $k = 10$. In this current characteristics, it is detected that the on-current (2.3×10^{-5}) rises by the rise in dielectric constant K . In proposed device drain current curve shows an improved I_{on}/I_{off} ratio (0.2×10^{11}) and minimum subthreshold swing (63 mV/decade) are obtained. This is for change in the dielectric, a BTBT is happening vertically to the gate oxide in adding to the tunnelling region due to the occurrence of charge plasma. Similarly, the operation of greater work-function of gate material at the drain decreases the I_{off} -state current (1.381×10^{-17}). Then I_{off} - current be depending mostly on the electrons moving over barrier relatively than the tunneling region. Further, the expansion in subthreshold swing. Hence, the complete current characteristics are detected to be better in the proposed device. The conduction band energy diagram shown in Fig. 3 can validate the above outcome.

The reaction of these biosensors with neutral charge density is examined in relations to sensitivity. In this case that the nanogap region is unfilled with biomolecules or filled with biomolecules is designated. Moreover, a position of the biosensors has the capability to return the reaction of the sensor by sensing objects. Figure 7(a) and (b) shows the sensitivity, along with dissimilar biomolecules and variation of charge densities, for the proposed device. It is observed that the sensitivity rises with the rise in biomolecules as K 's shows extreme detected at biomolecules as $K = 10$ is improved in the proposed device. Hence, the proposed device can be qualified to the improved charge plasma and improved schottky tunnelling tolerating for much- enhanced I_{on} - I_{off} ratio. Furthermore, the significance, of variation in on-state current rises and, hence, raises the sensitivity of the device. In the case of negative charge density, the reduction in sensitivity with the rise in the amount of ρ , regardless of the K 's significance. Lesser sensitivity at upper ρ is detected due to a quite minor variation in I_{on} of the device. The cause of reduced charge plasma and large tunneling width decreases the field release module of the total drain current. Hence, this results decreases of the I_{on} and finally the sensitivity of the device.

Figure 8(a) shows the impact of negative charges on threshold voltage using charge plasma based SB-FET as biosensor by taking $k = 1, 4, 10,$ and 12 . In this the charge of immobilized biomolecules fluctuates from low to $-10 \times 10^{11} \text{ cm}^{-3}$, the drain current is moved to the right. This relates to the rise in threshold voltage which can be detected from Fig. 8(a). Though, for a particular value of negative charge, the threshold voltage knowingly decreases with the rise in dielectric constant. In Fig. 8(b) shows the decline of threshold voltage with the rise in the amount of positive charges. For a certain value of a positive charge, threshold voltage reduces with the growing value of the dielectric constant.

Conclusion

The proposed charge plasma based dielectric variation of SB-FET as biosensor section has been considered in this device. The nanogap regions are designed in the device by removing out the gate-dielectric below the gate region to detect the positive and negative charged biomolecules. The charge density and dielectric constant related to the biomolecules modify the connection among source-channel interfaces. This results controls the schottky thickness near the source/Si-channel interface. In a variation of dissimilar dielectrics, and the charge density, on schottky barrier tunneling of electrons rate, drain current, electrostatic potential, and sensitivity were examined. Moreover, by detecting the sensing ability of the proposed biosensor is considered superior for the neutral and the charged biomolecules. Also, due to the use of charge plasma, low doping silicon, and decreased doping variations outcome and can be processed at a lower thermal budget.

Declarations

Funding statement: Funding information is not applicable

Conflict of Interest: No conflict of interest

Author contributions: All the authors are involved in review on the schottky barrier FET and Simulation and Analysis of the device.

Availability of data and material: There is no any other data and material associated with this manuscript.

Compliance with ethical standards: The author declare that he has no known competing financial interests or personal relationships that could have appeared to influence the work reported in this paper.

The author declare that there is no conflict of interest.

Consent to participate: Not applicable.

Consent for Publication: Not applicable as the manuscript does not contain any data from individual.

References

1. K. S. Min *et al.*, "A novel damage-free high-k etch technique using neutral beam-assisted atomic layer etching (NBALE) for sub-32nm technology node low power metal gate/high-k dielectric CMOSFETs," in 2009 IEEE International Electron Devices Meeting (IEDM), Baltimore, MD, USA, Dec. 2009, pp. 1–4, doi: 10.1109/IEDM.2009.5424330.
2. J. M. Kinsella and A. Ivanisevic, "Biosensing: Taking charge of biomolecules," *Nat. Nanotechnol.*, vol. 2, no. 10, pp. 596–597, Oct. 2007.
3. Narang R, Reddy KVS, Saxena M, et al (2012) A Dielectric-Modulated Tunnel-FET-Based Biosensor for Label-Free Detection: Analytical Modeling Study and Sensitivity Analysis. *IEEE Trans Electron Devices* 59:2809–2817. <https://doi.org/10.1109/TED.2012.2208115>
4. P Kumar, and B Bhowmick (2018) Comparative Analysis of Hetero Gate Dielectric Hetero Structure Tunnel FET and Schottky Barrier FET with n+ Pocket Doping for Suppression of Ambipolar Conduction and Improved RF/Linearity. *J. Nanoelectron. Optoelectron* <https://doi.org/10.1166/jno.2018.2488>
5. Narayanan V, Liu Z, Shen Y-MN, et al (2000) Reduction of metal-semiconductor contact resistance by embedded nanocrystals. In: *International Electron Devices Meeting 2000. Technical Digest. IEDM (Cat. No.00CH37138)*. IEEE, San Francisco, CA, USA, pp 87–90
6. Saitoh W, Itoh A, Yamagami S, Asada M (1999) Analysis of Short-Channel Schottky Source/Drain Metal-Oxide-Semiconductor Field-Effect Transistor on Silicon-on-Insulator Substrate and Demonstration of Sub-50-nm n-type Devices with Metal Gate. *Jpn J Appl Phys* 38:6226–6231. <https://doi.org/10.1143/JJAP.38.6226>
7. Lee I, Kim JN, Kang WT, et al (2020) Schottky Barrier Variable Graphene/Multilayer-MoS₂ Heterojunction Transistor Used to Overcome Short Channel Effects. *ACS Appl Mater Interfaces* 12:2854–2861. <https://doi.org/10.1021/acsami.9b18577>
8. Fernández AF, Zojer K (2017) Utilizing Schottky barriers to suppress short-channel effects in organic transistors. *Appl Phys Lett* 111:173302. <https://doi.org/10.1063/1.4997405>
9. Sadighbayan D, Hasanzadeh M, Ghafar-Zadeh E (2020) Biosensing based on field-effect transistors (FET): Recent progress and challenges. *TrAC Trends in Analytical Chemistry* 133:116067. <https://doi.org/10.1016/j.trac.2020.116067>
10. Masurkar N, Varma S, Mohana Reddy Arava L (2020) Supported and Suspended 2D Material-Based FET Biosensors. *Electrochem* 1:260–277. <https://doi.org/10.3390/electrochem1030017>
11. Kumar P, Wasim Arif, Bhowmick B (2018) Scaling of Dopant Segregation Schottky Barrier Using Metal Strip Buried Oxide MOSFET and its Comparison with Conventional Device. *Silicon* 10:811–820. <https://doi.org/10.1007/s12633-016-9534-5>
12. Prashanth Kumar, Brinda Bhowmick (2017) 2-D analytical modeling for electrostatic potential and a threshold voltage of a dual work function gate Schottky barrier MOSFET. *J Comput Electron*. <https://doi.org/10.1007/s10825-017-1011-x>
13. Lee S (2017) Electrodes for Semiconductor Gas Sensors. *Sensors* 17:683. <https://doi.org/10.3390/s17040683>

14. Hafiz SA, Iltesha, Ehteshamuddin M, Loan SA (2019) Dielectrically Modulated Source-Engineered Charge-Plasma-Based Schottky-FET as a Label-Free Biosensor. *IEEE Trans Electron Devices* 66:1905–1910. <https://doi.org/10.1109/TED.2019.2896695>
15. Abdi DB, Kumar MJ (2015) Dielectric modulated overlapping gate-on-drain tunnel-FET as a label-free biosensor. *Superlattices and Microstructures* 86:198–202. <https://doi.org/10.1016/j.spmi.2015.07.052>
16. Kumar P, Bhowmick B (2017) 2D analytical model for surface potential based electric field and impact of work function in DMG SB MOSFET. *Superlattices and Microstructures* 109:805–814. <https://doi.org/10.1016/j.spmi.2017.06.001>
17. Kumar P, Bhowmick B A physics-based threshold voltage model for hetero-dielectric dual material gate Schottky barrier MOSFET. *Int J Numer Model* <https://doi.org/10.1002/jnm.2320>.
18. Hafiz SA, Iltesha, Ehteshamuddin M, Loan SA (2019) Dielectrically Modulated Source-Engineered Charge-Plasma-Based Schottky-FET as a Label-Free Biosensor. *IEEE Trans Electron Devices* 66:1905–1910. <https://doi.org/10.1109/TED.2019.2896695>
19. Atlas User's Manual: Device Simulation Software, Silvaco Int., Santa Clara, CA, USA, 2008.
20. Jhaveri R, Nagavarapu V, Woo JCS (2009) Asymmetric Schottky Tunneling Source SOI MOSFET Design for Mixed-Mode Applications. *IEEE Trans Electron Devices* 56:93–99. <https://doi.org/10.1109/TED.2008.2008161>.
21. Kumar P, Bhowmick B (2018) Suppression of ambipolar conduction and investigation of RF performance characteristics of gate-drain underlap SiGe Schottky barrier field effect transistor. *Micro & Nano Letters* 13:626–630. <https://doi.org/10.1049/mnl.2017.0895>
22. Kale S, Kondekar PN (2017) Design and Investigation of Dielectric Engineered Dopant Segregated Schottky Barrier MOSFET With NiSi Source/Drain. *IEEE Trans Electron Devices* 64:4400–4407. <https://doi.org/10.1109/TED.2017.2754881>
23. Prashanth Kumar, A Vinod, Krishna D, Brinda B “Analysis and Simulation of Schottky Tunneling using Schottky Barrier FET with 2-D Analytical Modeling”, Volume 107, Silicon, JAN 2021
24. P Kumar B. Bhowmick, A Vinod “Impact of Ferroelectric on the Electrical Characteristics of Silicon–Germanium based heterojunction Schottky Barrier MOSFET”, doi.org/10.1016/j.aeue.2019.05.030 ISSN-1434-8411 Volume 107, Pages 257-263 AEU, May 2019
25. P. Kumar and B. Bhowmick, “Source-Drain Junction Engineering Schottky Barrier MOSFETs and their Mixed Mode Application,” *Silicon*, vol. 12, no. 4, pp. 821–830, Apr. 2020, doi: 10.1007/s12633-019-00170-0. *Silicon*, 2019

Figures

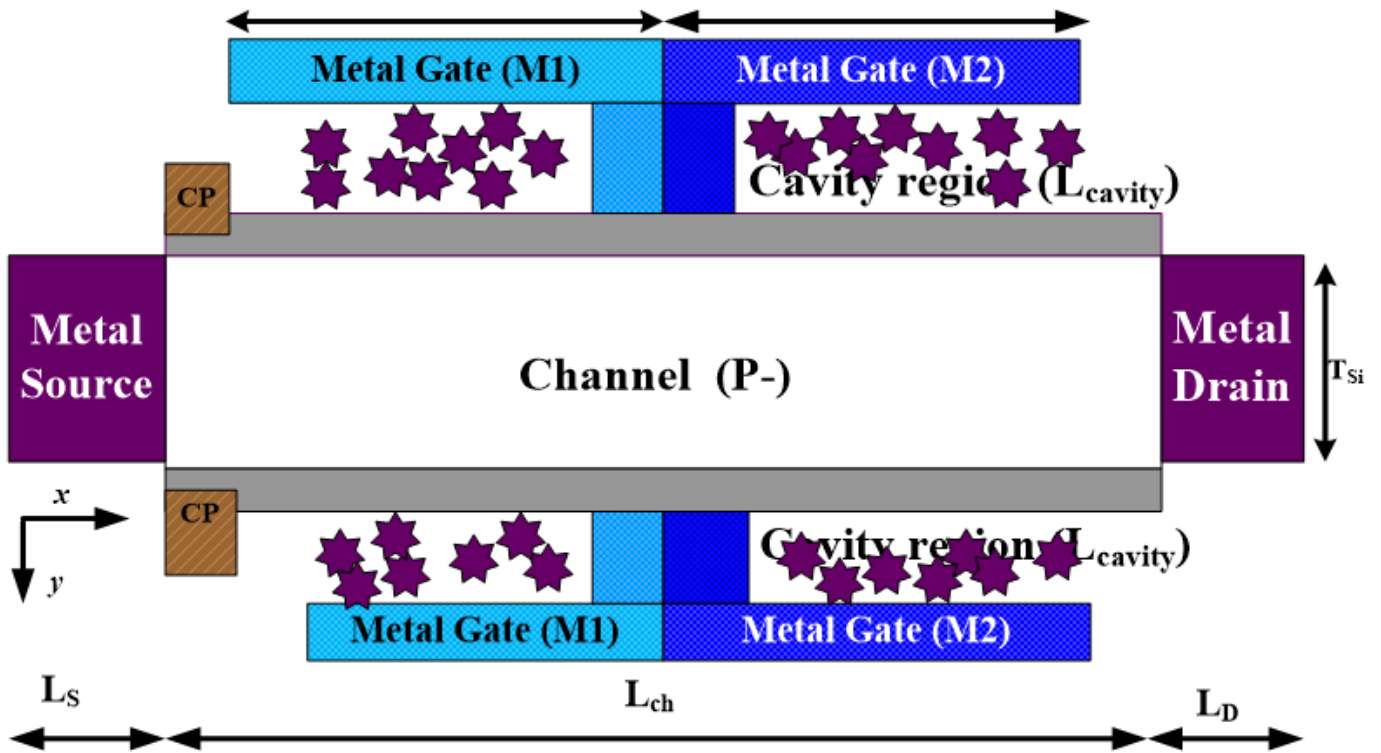


Figure 1

Charge-plasma based dielectric modulated SB-FET biosensor

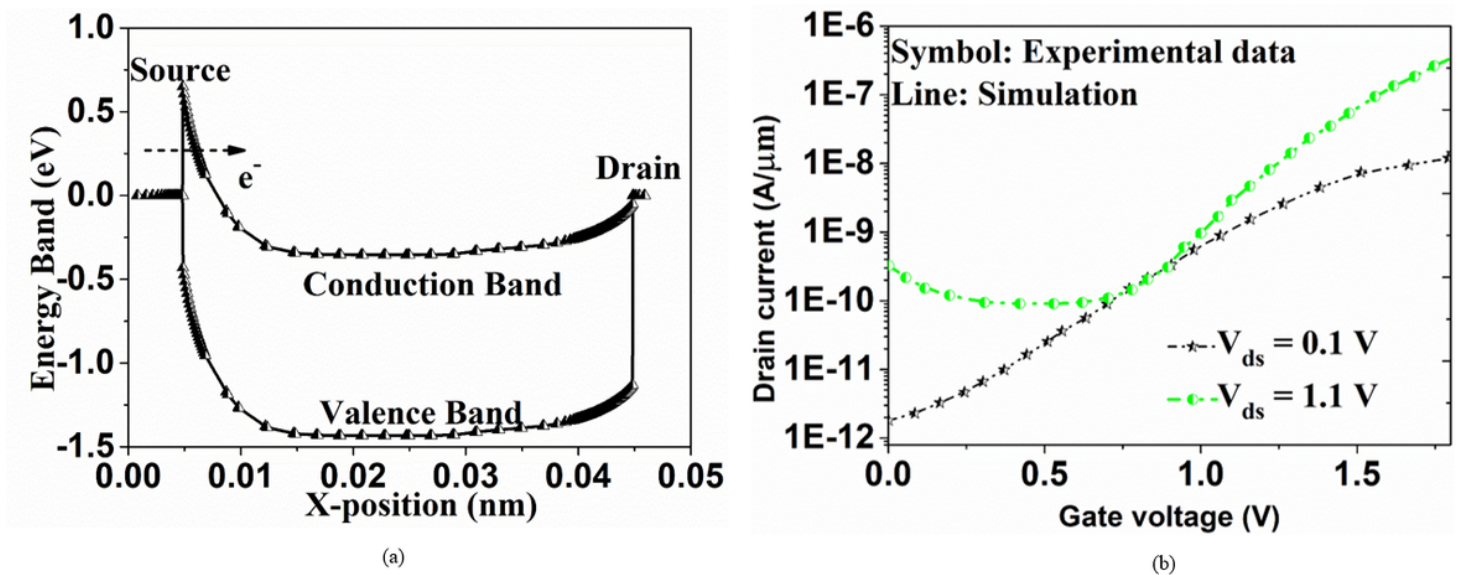


Figure 2

(a) Energy band diagrams of the Charge plasma based dielectric variation -SB-FET along the device length in the on-state ($V_{gs} = 0.8$ V, $V_{ds} = 0.8$ V). (b) Transfer characteristics of experimental results of [20], compared with proposed device.

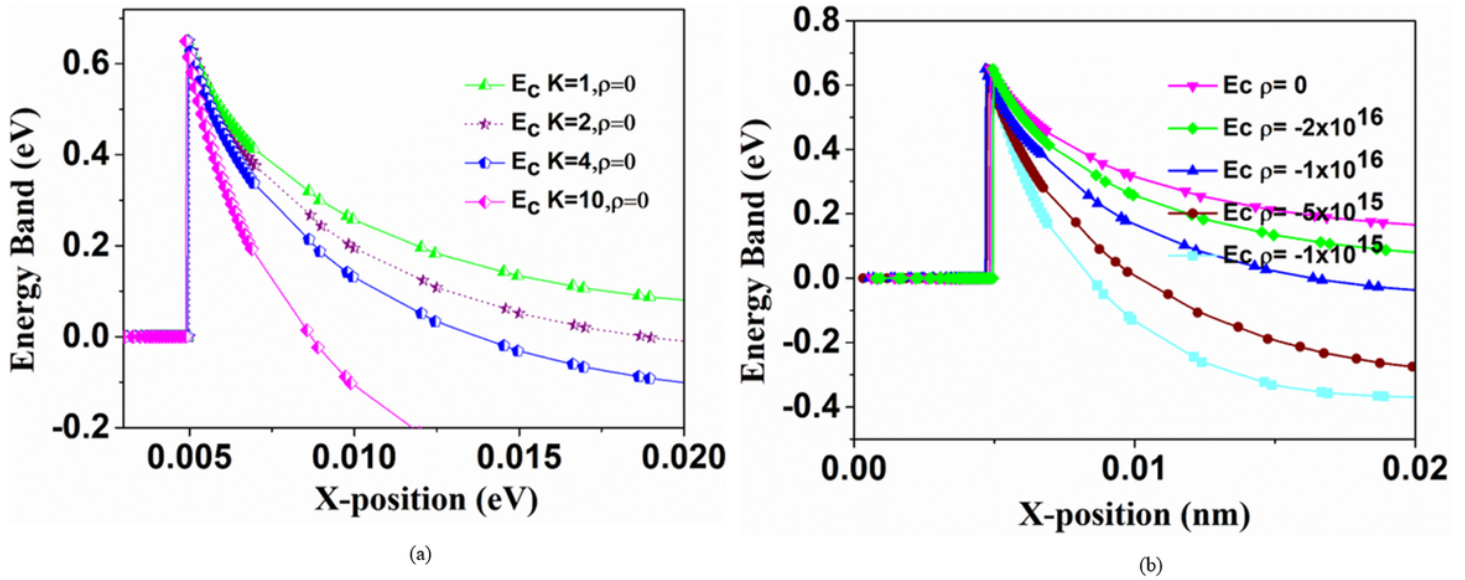


Figure 3

Conduction band for (a) change in dielectric constant as biomolecule at $V_{gs}= 0.8$ and $V_{ds}= 0.8$ V and (b) change in charge density (ρ) at $V_{gs}= 0.8$ and $V_{ds}= 0.5$ V.

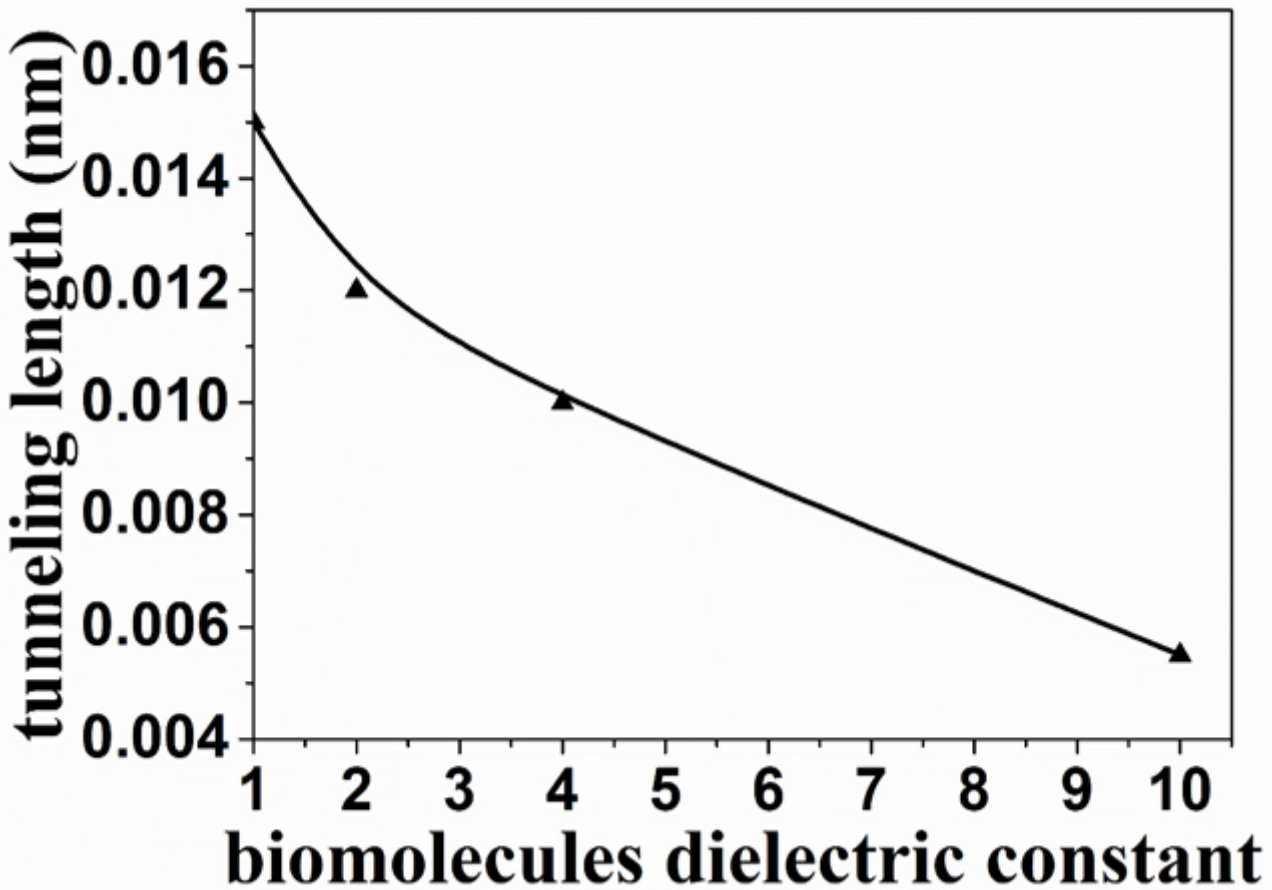


Figure 4

Variation of tunneling length along with dielectric constant.

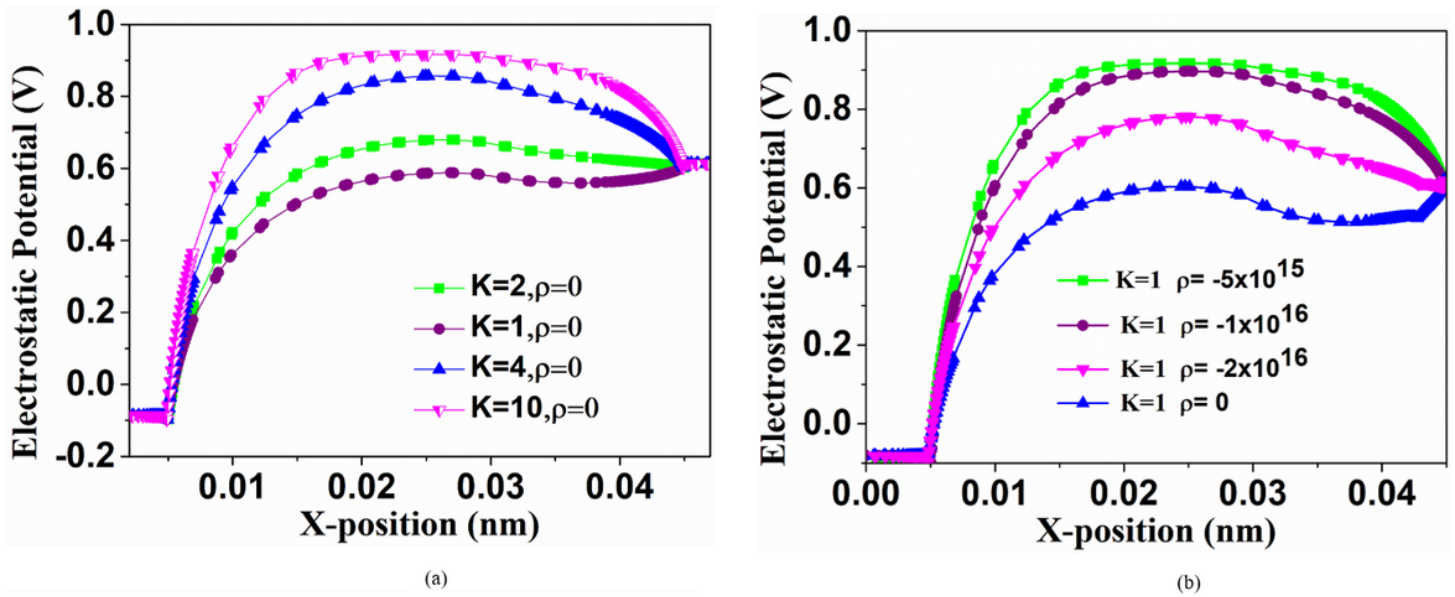


Figure 5

Variation of electrostatic potential sensitivity with different (a) dielectric constant ($\rho = 0$) (b) different charge densities, ρ , at $V_{ds} = 0.8$ V and $V_{gs} = 0.8$ V.

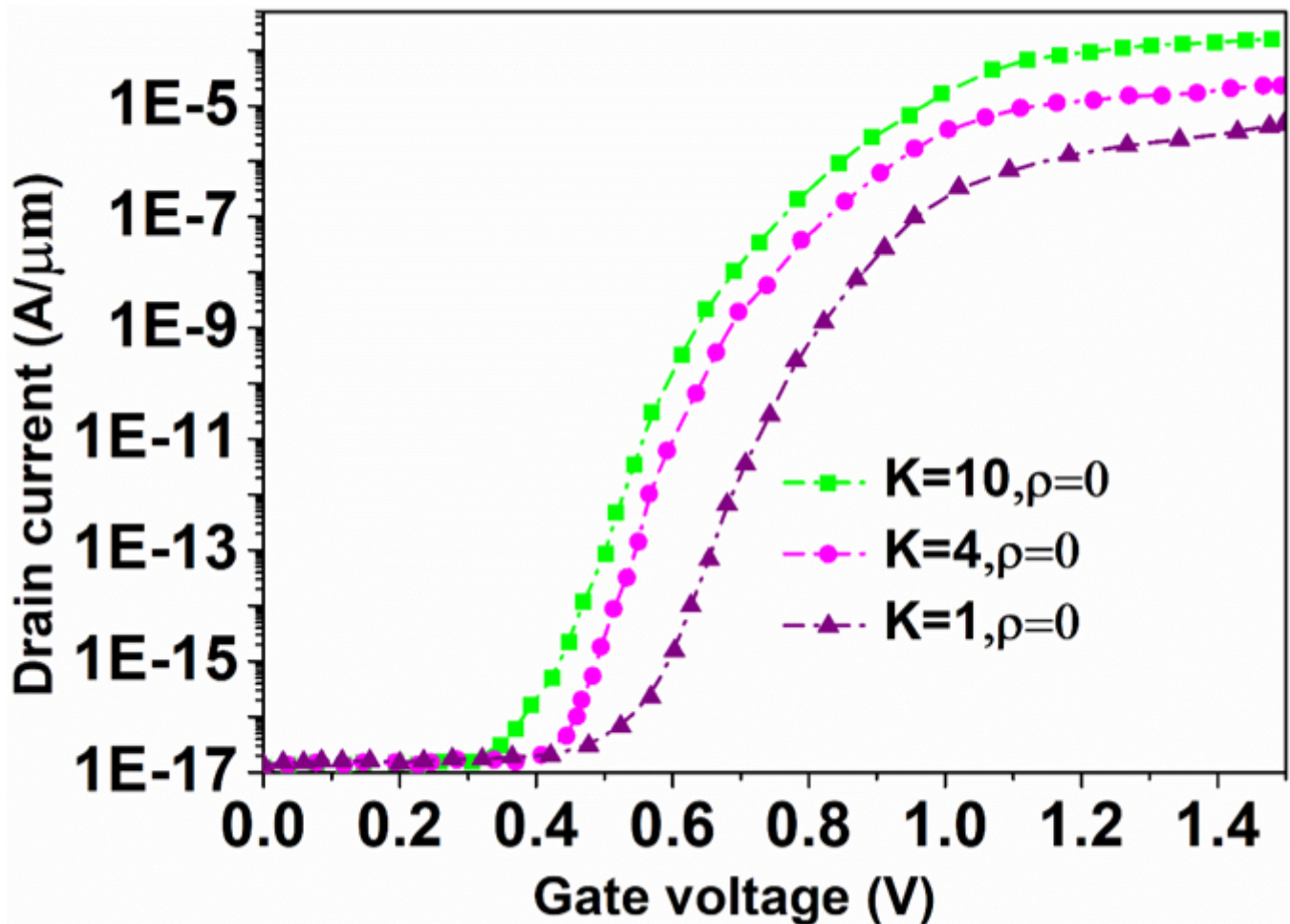


Figure 6

Transfer characteristics of the charge plasma based variation of -SB-FET as biosensor different dielectric constants, K's (at $\rho = 0$).

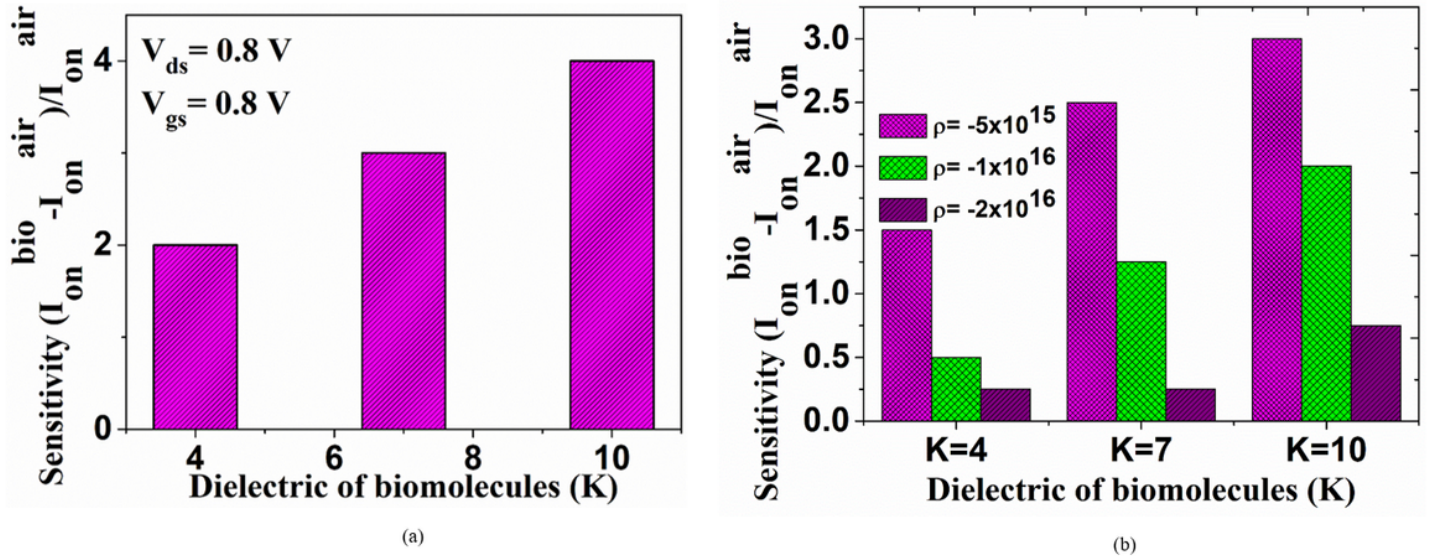


Figure 7

Sensitivity study of the charge plasma based SB-FET as biosensor at (a) different dielectric constants, K (at $\rho = 0$) (b) different charge densities, ρ

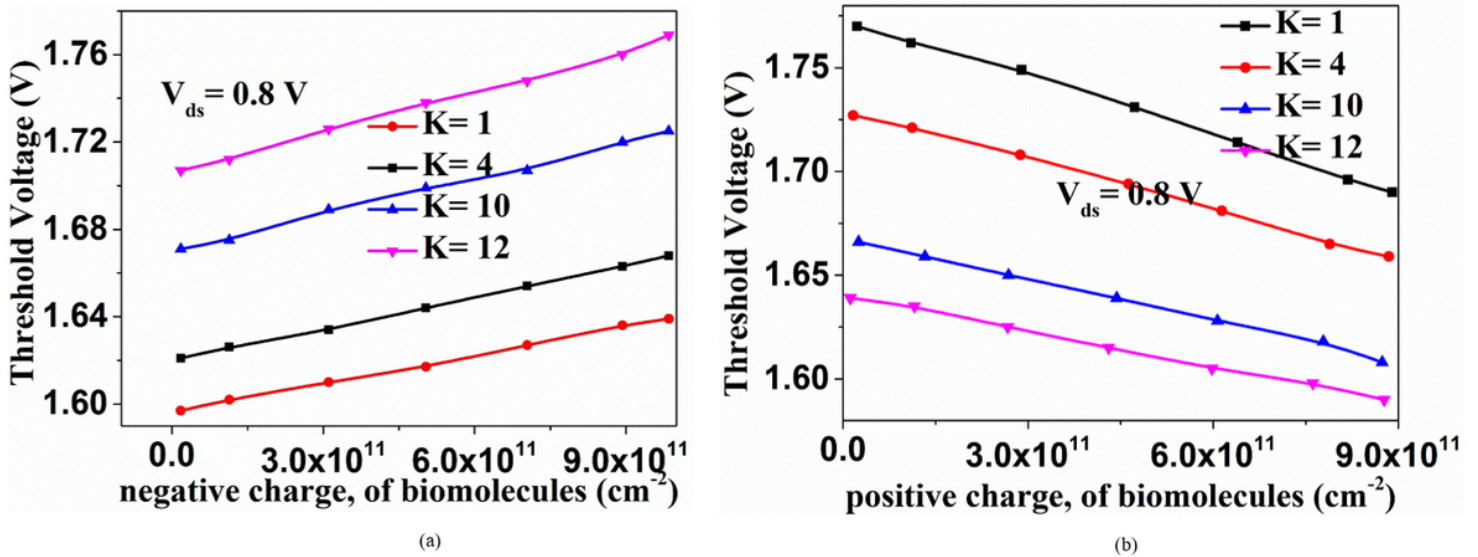


Figure 8

Threshold Voltage along with different dielectric constant, k = 1,4,10 and 12 for (a) negative charge of biomolecules for, (b) positive charge of biomolecules.